

# AN ANALYSIS OF THE VARIABILITY OF THE NORTH ATLANTIC OSCILLATION IN THE TIME AND THE FREQUENCY DOMAINS

D. POZO-VÁZQUEZ<sup>a,b,\*</sup>, M.J. ESTEBAN-PARRA<sup>b</sup>, F.S. RODRIGO<sup>c</sup> and Y. CASTRO-DÍEZ<sup>b</sup>

<sup>a</sup> *Departamento de Física, University of Jaén, E-23071, Jaén, Spain*

<sup>b</sup> *Departamento de Física Aplicada, University of Granada, E-18071, Granada, Spain*

<sup>c</sup> *Departamento de Física Aplicada, University of Almería, E-04120, Almería, Spain*

*Received 26 May 1999*

*Revised 23 February 2000*

*Accepted 24 February 2000*

## ABSTRACT

An analysis of the variability of the North Atlantic Oscillation (NAO) since the beginning of the 19th century has been carried out using monthly pressure series from Gibraltar, Lisbon, The Azores and Iceland. In the first part, the combinations of stations that best monitor the NAO at different time intervals (monthly, seasonal and winter-annual) are analysed based on a signal/noise approach. The stability through time of the relationship between the pressures at the different stations is also studied. Based on this analysis, proxy indices of the NAO are obtained and compared with the NAO index resulting from a principal component analysis (PCA) of gridded sea level pressure (SLP) data. In the second part, the cross-spectral characteristics of the data of the northern and southern stations are studied in order to determine for which ranges of periods the pressure undergoes simultaneous coherent and out-of-phase variations. Based on the cross-spectral analysis, several filters are proposed to be applied to the pressure series prior to calculating the NAO index, in order to improve the reliability of the NAO index as an indicator of the NAO. Results show that for a monthly or seasonal index, The Azores must be selected as the southern station, but the strongest relationship is found for winter using Gibraltar as the southern station. The cross-spectral analysis shows, firstly, that the periods that are mainly responsible for coherent and out-of-phase variations are 6 months, 1 year, 2 years and 8 years (the most important). Secondly, several ranges of periods, mainly from 3 to 4 years and less than 6 months, are shown not to contribute to coherent and out-of-phase relationships between stations. Removing these ranges of periods from the pressure series prior to calculating the indices notably improves the reliability of the indices as indicators of the NAO state. The comparison of the filtered and unfiltered indices shows that extreme values of the NAO result from coherent out-of-phase pressure variations between stations. Copyright © 2000 Royal Meteorological Society.

KEY WORDS: cross-spectral analysis; NAO; North Atlantic

## 1. INTRODUCTION

Climates of different regions at the same latitude can be quite different, but low frequency variations (on interannual and longer time scales) of temperature and precipitation tend to occur in large spatial patterns often associated with changes in distinctive circulation phenomena (Trenberth, 1995). Among the several modes of low frequency variability in geopotential heights in the Northern Hemisphere, the most important one is known as the North Atlantic Oscillation (NAO) (Wallace and Gutzler, 1981; Barnston and Livezey, 1987). This is characterized by a north–south dipolar pattern of opposite sign anomalies, with one of the centres of the dipole located over Iceland and the other one, approximately, over The Azores. Although there are other patterns of variability, the NAO is the only one active throughout the entire year.

The NAO dipolar pattern shows a pronounced seasonal variation in its intensity, position and shape (Barnston and Livezey, 1987; Mächel *et al.*, 1998). For instance, during winter (mainly in November and

\* Correspondence to: Departamento de Física Aplicada, Universidad de Granada, 18071, Granada, Spain; e-mail: dpozo@ugr.es

December) there are two centres in the south, one over the Atlantic and the other one over the eastern Mediterranean region, while in summer the latter centre becomes weaker and disappears. The dipole undergoes a northward displacement in summer and a southward displacement in winter (as those undergone by the westerlies as a consequence of the annual solar cycle). Because of the greater vigour of the circulation during the winter season, in coincidence with the greater temperature gradient from the equator to the poles, the NAO pattern is most pronounced both in intensity and in area coverage during the winter (Moses *et al.*, 1987), in which it accounts for around one-third of the total sea level pressure (SLP) field variance (Wallace and Gutzler, 1981; Barnston and Livezey, 1987). The NAO reflects the strong meridional pressure contrast in the North Atlantic region, with a low-pressure centre in the north over Iceland and a high-pressure centre over The Azores islands. Changes in pressure at these two centres tend to occur out-of-phase.

Together with the variability in the position and shape of the dipole, the NAO presents a remarkable interannual variability that can be summarized in two phases: the positive phase of the NAO reflects below-normal heights and pressure across the high latitudes of the North Atlantic, as well as above-normal heights and pressure over the central North Atlantic; the negative phase indicates an opposite pattern of height and pressure anomalies. Both phases of the NAO are associated with basin-wide changes in the intensity and location of the North Atlantic jet stream, storm track and changes in the patterns of zonal and meridional heat and moisture transport from the Atlantic ocean to the continental areas of Europe (Hurrell, 1995, 1996; Hurrell and van Loon, 1997). This results, for the positive phase, in an intensified westerly flow that brings warm maritime air to Europe during winter, reducing the polar outbreaks over Europe, leading to a warming of central and southern Europe and a cooling of the northwestern Atlantic (Rogers and van Loon, 1979; Hurrell, 1996; Kapala *et al.*, 1998; Osborn *et al.*, 1999). With respect to precipitation, the positive phase is associated with positive anomalies in northern Europe and negative anomalies in central and southern Europe. When the NAO is negative, opposite patterns of precipitation and temperature anomalies are to be found.

The NAO mode of variability of pressure in the North Atlantic is found when a principal component analysis (PCA) of SLP is carried out. However, pressure data over the entire North Atlantic area are available only for a short time period. A proxy technique to monitor the NAO and to study its temporal variability back in time is by means of an index. The index is constructed using the pressure differences between a station located near the southern centre of the dipole and the other one near the northern centre. In recent years, several NAO proxy indices have been proposed using different stations and different time-averaged intervals of the year (Hurrell and van Loon, 1997; Jones *et al.*, 1997). In the present work, an analysis was made of NAO proxy indices at monthly, seasonal and winter-annual time scales. The work is divided in two parts. The first part is concerned with the feasibility of using the NAO index to monitor the NAO for each month of the year. An analysis is performed to select the individual station (among those available) that would best represent the southern part of the NAO dipole for different time scales and time of the year. The indices constructed are compared with the NAO index that was defined by Barnston and Livezey (1987) on the basis of a PCA of gridded geopotential heights. In the second part, the indices calculated are analysed. Cross-spectral characteristics of the pressure data of the northern and southern stations are studied. The objective is to identify which frequency ranges contribute to coherent out-of-phase variations of the pressure at the southern and northern stations (i.e. those that are NAO signals). For improved statistical reliability of the results, when a statistically significant auto-correlation pattern is present in a series, correlation and cross-spectral analyses were performed using the residual of autoregressive integrated moving average (ARIMA) models fitted to the series (pre-whitening procedure). Based on this analysis, the use of digital filters is proposed to improve the reliability of the NAO index as an indicator of the NAO state.

In the appendix, a brief description of the methodologies used in this work, concerning ARIMA modelling, pre-whitening procedure and cross-spectral analysis, is given. Section 2 describes the data used. Section 3 contains the analysis. Finally, some conclusions are given in Section 4.

## 2. DATA

The pressure data analysed correspond to Gibraltar (GI hereafter) (36.1°N, 5.4°W) and southwestern Iceland (IC hereafter), the latter comprised mainly of data from Reykjavik and Stykkisholmur (65.0°N, 22.8°W), (Jones *et al.*, 1997). Data from The Azores islands (AZ hereafter) (Ponta Delgada, 37.7°N, 25.7°W) (Jones *et al.*, 1987) and Lisbon (LI hereafter) (38.7°N, 9.15°W) (Hurrell, 1995) have been also used. The records are on a monthly basis, extending from 1865 to 1997 for AZ and LI and from 1825 to 1997 for GI and IC.

Table I shows the mean and standard deviations of the pressure at GI, AZ, LI and IC, for different time-averaged intervals, for the period of normalization 1951–1980. Firstly, note that the standard deviation in Iceland is greater than those for the southern part of the dipole. The annual cycle both in the means and standard deviations is also remarkable. The final purpose is to establish an NAO index comparing the pressure data of two stations. Owing to the different statistical characteristics of the northern and southern stations, data (especially with respect to the standard deviation) and owing to the change of both mean and standard deviations throughout the year, a normalization process for each pressure time series is necessary in order to avoid creating a biased and misleading index. Thus, a monthly deseasonalized and normalized index is constructed for each station, which consists of calculating the difference between each raw monthly value and a time-averaged monthly mean value, and then dividing by a time-averaged monthly standard deviation. Note that this process removes the seasonal cycle. Normalization relative to the period 1951–1980 has been used. Although other normalization procedures have been proposed (Ropelewski and Jones, 1987), this has been upheld as the optimal one (Trenberth, 1984). Following this procedure, a seasonal index for each station is constructed using averages of three consecutive monthly pressure values and their corresponding seasonal and standard deviation long-term mean values (December–February for winter, etc.). Due to the selected normalization period, the indices do not have a mean of zero and a standard deviation of unity.

Table I. Monthly and seasonal mean and standard deviation (S.D.) in mb of SLP at GI, AZ, LI and IC. The normalization period 1951–1980 has been used

	GI		AZ		IC		LI	
	Mean	(S.D.)	Mean	(S.D.)	Mean	(S.D.)	Mean	(S.D.)
Months								
Jan	1020.8	3.1	1019.0	6.1	1001.6	9.5	1019.5	4.2
Feb	1019.6	3.6	1018.4	6.5	1004.3	8.2	1018.0	4.2
Mar	1018.1	3.3	1018.3	4.8	1005.4	7.4	1016.9	3.6
Apr	1016.6	1.8	1021.3	3.6	1010.0	4.4	1016.1	2.5
May	1016.9	1.4	1022.5	2.7	1013.4	5.5	1017.0	2.4
Jun	1017.4	1.1	1024.1	2.2	1010.0	3.9	1017.4	1.7
Jul	1016.9	0.9	1025.3	1.9	1010.1	3.6	1017.7	1.3
Aug	1016.1	0.9	1023.1	1.8	1008.9	3.4	1017.1	1.4
Sep	1017.7	1.0	1022.0	2.4	1005.4	4.8	1017.8	1.8
Oct	1018.3	2.1	1019.6	2.5	1002.2	6.2	1017.5	2.9
Nov	1019.2	2.4	1020.3	3.4	1003.2	6.6	1018.3	2.8
Dec	1020.2	3.0	1021.5	4.4	1000.3	7.9	1019.7	4.3
Seasons								
DJF	1020.1	2.1	1019.5	3.5	1002.1	5.5	1019.2	3.1
MAM	1017.2	1.4	1020.7	1.9	1009.6	3.4	1016.7	1.6
JJA	1016.8	0.5	1024.1	1.3	1009.7	2.3	1017.4	1.3
SON	1018.4	1.1	1020.6	1.4	1003.6	3.8	1018.0	2.3

### 3. ANALYSING THE DATA

As pointed out above, the NAO signal is characterized by an out-of-phase relationship between the variations of the pressure at the northern and southern centres of the dipole. A simple index composed of the southern minus the northern station index can be used to represent the NAO signal, however, bearing in mind that:

- (i) the selected stations must be representative of the two centres of action of the NAO;
- (ii) besides the NAO, other meteorological phenomena, not related at all to it, affect the pressure measured at a particular station.

Thus, to obtain a meaningful index of the NAO through a comparison of the pressure anomalies of two places we must (i) choose the two stations as near as possible to the two centres of action; (ii) try to construct an index that mainly retains the simultaneous out-of-phase pressure variations that take place at both stations. We deal with these two problems in this section.

To monitor the performance of the index as an indicator of the NAO a signal-to-noise ratio ( $S/N$  hereinafter), such as those defined by Trenberth (1984), can be used. The ratio is determined as follows:

$$(S/N) = [(1 - r_{12})/(1 + r_{12})]^{1/2},$$

where  $r_{12}$  stands for the correlation coefficient between stations 1 and 2; and  $1 - r_{12}$  and  $1 + r_{12}$  represent, respectively, the standard deviation of  $(S_1 - S_2)$  and  $(S_1 + S_2)$  signals,  $S_i$  being the normalized pressure anomaly (monthly, seasonal or annual) at station  $i$ . Since NAO is characterized by an out-of-phase relationship between two stations,  $(S_1 - S_2)$  could be used as an indicator of the NAO signal (since it will enhance out-of-phase relationships) and  $(S_1 + S_2)$  could be used to measure the noise in the NAO; i.e. all the fluctuations between the two action centres that occur in phase or almost in phase are, therefore, not part of the NAO signal. A high value of the  $S/N$  ratio would indicate that the index adequately monitors the NAO, while an index with a low  $S/N$  ratio can be used only with care as an NAO indicator, since it contains considerable non-NAO signals.

#### 3.1. Analysis of the relationship between stations

The NAO spatial pattern undergoes changes, both in position and shape, throughout the year and most probably with the period of analysis (Barnston and Livezey, 1987; Davis *et al.*, 1997; Mächel *et al.*, 1998). For instance, the southern centre of the dipole, during the Northern Hemisphere winter, is located in a more southeasterly position than in spring and summer because of the clockwise migratory pattern which the sub-tropical high follows throughout the year. The northern centre of the dipole is more stable in its position over the year, and Icelandic pressure can adequately account for its behaviour (Shasmanoglou, 1990).

The nearest station to the southern centre of action of the NAO can be chosen by studying the correlation between the three southern stations and the northern station. A highly negative correlation would indicate a strong out-of-phase relationship between stations. This analysis has been made using the anomaly indices resulting from the normalization process summarized above. In some cases, residual time-series resulting from the ARIMA model applied to the index, instead of the index itself, were used. This procedure ensures a better estimate of the relationship between time series (see Appendix A: pre-whitening).

Table II shows the  $S/N$  and the correlation between pressure indices of the different stations, for the complete study period. During winter, GI appears to be nearer than AZ to the southern centre of the dipole ( $S/N$  is 2.17 for GI–IC in comparison with 2 for AZ–IC), in agreement with the migratory pattern followed by the sub-tropical high throughout the year. Values for LI are very similar to those of GI ( $S/N$  is 2.13 for winter). February shows the highest coherence between the northern and southern stations.

Stability of these relationships throughout the period analysed has been studied. Figure 1(a) shows the correlation of the pressure indices of GI and IC, LI and IC, and AZ and IC in winter, computed over a

Table II. *S/N* and correlation between the normalized pressure anomalies of GI-IC, AZ-IC and LI-IC; correlation between the normalized pressure anomalies of GI-AZ, LI-AZ and GI-LI

	GI-IC		AZ-IC		LI-IC		GI-AZ	LI-AZ	GI-LI
	Correlation	<i>S/N</i>	Correlation	<i>S/N</i>	Correlation	<i>S/N</i>	Correlation	Correlation	Correlation
Month									
Jan	-0.54	1.83	-0.58	1.94	-0.52	1.78	0.54	0.70	0.94
Feb	-0.65	2.17	-0.57	1.91	-0.65	2.17	0.62	0.77	0.93
Mar	-0.58	1.94	-0.63	2.10	-0.63	2.10	0.53	0.67	0.91
Apr	-0.26	1.30	-0.50	1.73	-0.34	1.42	0.31	0.48	0.80
May	-0.12	1.13	-0.43	1.58	-0.17	1.19	0.28	0.28	0.48
Jun	-0.07	1.07	-0.46	1.64	-0.01	1.01	0.29	0.38	0.54
Jul	-0.07	1.07	-0.34	1.42	-0.05	1.05	0.18	0.18	0.31
Aug	-0.07	1.07	-0.41	1.55	-0.14	1.15	0.10	0.23	0.42
Sep	-0.14	1.15	-0.51	1.76	-0.19	1.21	0.14	0.22	0.58
Oct	-0.32	1.39	-0.51	1.76	-0.30	1.36	0.26	0.50	0.75
Nov	-0.38	1.49	-0.50	1.73	-0.40	1.53	0.37	0.49	0.88
Dec	-0.59	1.97	-0.49	1.71	-0.56	1.88	0.43	0.59	0.93
Seasons									
DJF	-0.65	2.17	-0.60	2.00	-0.64	2.13	0.63	0.73	0.92
MAM	-0.31	1.38	-0.58	1.94	-0.39	1.51	0.38	0.53	0.65
JJA	0.12	0.89	-0.36	1.46	0.05	0.95	0.21	0.31	0.21
SON	-0.26	1.30	-0.52	1.78	-0.29	1.35	0.35	0.45	0.70

The analysed period is 1825–1997 for the correlation of GI and IC, and 1865–1997 for the rest of the cases. S.D. of the correlation estimates are 0.09 for the case GI-IC and 0.08 the rest of the cases. In general, AZ has a more stable correlation with IC than with GI throughout the year, but the strongest relationship between the southern and northern stations appears in winter using GI as the southern station.

sliding window spanning 50 years (a standard error 0.14 for the estimates can be assumed). Figure 1(b) shows the corresponding *S/N* ratios. Overall, correlation using GI as the southern station is higher (more negative). Only during the last part of the record does LI show a slightly better correlation. Differences are especially pronounced in the period 1900–1940, in which correlation is  $-0.65$  using GI and  $-0.50$  using AZ or LI. Values for LI and GI are very similar during the first part of the record. These differences can be partially explained by taking into account that during the period 1900–1960, the Azores High was located in a more southerly position with respect to its long-term average position (Mächel *et al.*, 1998). From 1940 onwards, a trend toward higher correlation values (more negative) are found and correlations are similar using GI, AZ or LI as the southern centre for the dipole. The longest record available for GI, in comparison with those available for the pressure in AZ, and the results from the previous analysis indicate that the southern centre of the NAO dipole is better represented by GI than by AZ or LI pressure during winter.

Correlation between the northern and southern stations begins to decrease in April and reaches minimum values in summer (as might be expected by the lesser intensity of the NAO during this period). The migratory pattern followed by the Azores High accounts for the fact that from April to November the correlation is higher using AZ than using GI or LI. Particularly, in summer, the Azores High is located in its most westerly position, over The Azores islands. During these months, AZ pressure must be used as the proxy indicator of the southern centre of the NAO dipole. Figure 2 shows the correlation between AZ and IC pressure (computed using a sliding window spanning 50 years) for spring, summer and autumn (a standard error 0.14 for the estimates can be assumed). Spring correlation values have been

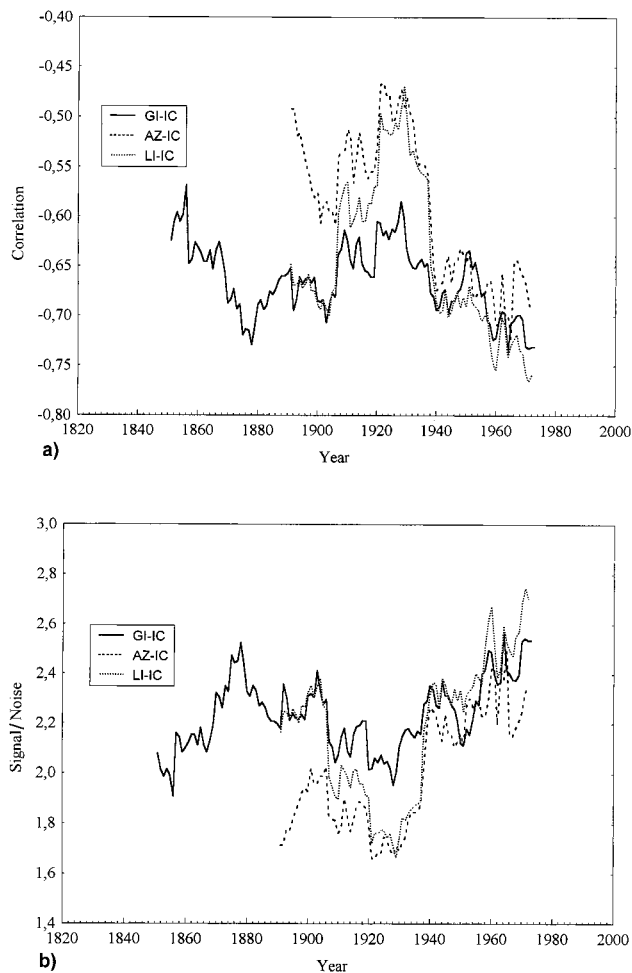


Figure 1. (a) Correlation between pressure during winter (DJF): GI-IC, solid line; AZ-IC, broken line; LI-IC, dotted line. Values have been computed over a sliding window spanning 50 years. A standard error of 0.14 can be assumed. (b) As in (a) but for the  $S/N$  ratio

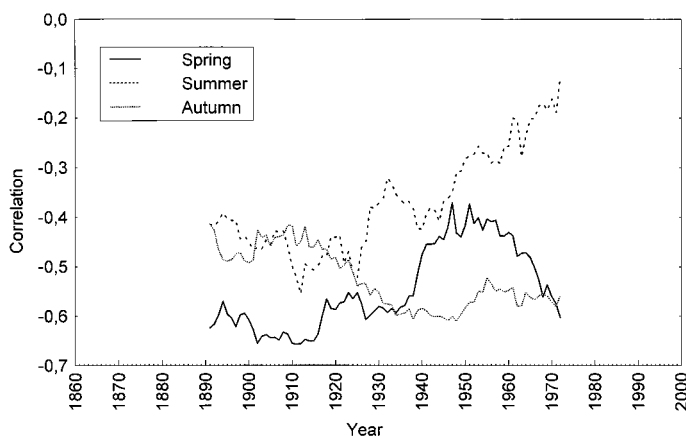


Figure 2. Correlation between the pressure at AZ and IC during spring, summer and autumn. Values have been computed over a sliding window spanning 50 years. A standard error of 0.14 can be assumed

quite stable throughout the period analysed, with only the period 1940–1965 showing lower values ( $-0.4$  in comparison with  $-0.6$  of the preceding decades). An analysis using a 25-year sliding window (not shown) indicates that the trend during the latest decades is toward values of around  $-0.6$ , as at the beginning of the record. Autumn also shows a quite stable correlation value of  $-0.5$ . A trend towards higher values (more negative correlation) appears from 1920 onwards. The most remarkable change in the correlation occurs in summer. During the period 1880–1930, the correlation value is  $-0.4$ , and from 1920 onwards there is a trend toward lower values (less negative correlation), reaching a value of  $-0.2$  during the period 1950–1970. An analysis using a 25-year sliding window confirms that this trend persists during the last two decades. A decreasing pressure gradient in summer, from 1960 onwards, between the Azores High and the Icelandic Low has been reported by Mächel *et al.* (1998). These researchers also found a northern displacement of the position of the Azores High in the period 1950–1990. These two factors can contribute to explaining the lower correlation found in the latter part of the record.

In short, the highest (most negative) value for the correlation between the southern and northern stations appears in winter, when the NAO signal is strongest, using GI as the southern station. However, if a monthly, seasonal or annual-averaged index is to be obtained, AZ must be selected as the southern station because of the low correlation between GI and IC during the summer months. In general, AZ has a more stable correlation with IC than GI and LI throughout the year. Our results closely agree with those of Hurrell and van Loon (1997) using pressure data of LI, Stykkisholmur and AZ from 1894 to 1995. The use of GI instead of Lisbon enables the period of analysis to be extended back in time until 1825.

As a result of this analysis, a monthly NAO index is obtained using the monthly-normalized pressure indices of AZ and IC. Similarly, a seasonal index is calculated using AZ, but based on seasonally averaged pressure. Both monthly and seasonal indices extend from 1865 to 1997. Finally, since the NAO is most pronounced in winter (and its influence strongest) and given that during this part of the year GI better represents the southern centre of the oscillation, a winter-annual index using GI as the southern station is calculated for the period 1825–1997.

### 3.2. Comparison with the original definition of NAO

In order to contrast the ‘real’ NAO with its proxy indices, we now compare the seasonal indices obtained in the previous section with the series of the NAO mode of variability obtained by Barnston and Livezey (1987), PC index thereafter. This index is the result of a PCA of SLP and is available from 1951 to 1997. Seasonal values have been obtained, based on monthly data, following the same normalization procedure used for the pressure series. Table III shows the correlation between the PC NAO index and the proxy indices obtained using AZ and IC and GI and IC. During winter, the proxy NAO index obtained using GI as the southern station has the greatest correlation with the PC index, while during the other seasons of the year AZ has a greater correlation. Note that the best correlation between the PC NAO index and the proxy indices is found during winter, followed by autumn and spring. Values are particularly low and negative during summer. Results must be treated with caution due to the short length of the comparison period (47 years).

Table III. Correlation between the NAO index as defined by Barnston and Livezey (1987) and the NAO index obtained using GI and AZ

Seasons	PC–GI	PC–AZ
DJF	0.91	0.89
MAM	0.06	0.44
JJA	−0.27	−0.21
SON	0.21	0.53

Seasonal values have been used. Standard deviation of the correlation estimates is 0.15.

### 3.3. Cross-spectral analysis and filtering

Even assuming that we have selected the stations nearest to the two centres of action, a NAO index constructed simply by subtracting anomalies still must be used with care to monitor the NAO. Each station undergoes changes in pressure due to transient short-term meteorological phenomena or, in general, phenomena not related to the NAO. A simple difference partially removes coherent-in-phase signals at both stations and enhances out-of-phase signals, but cannot remove other signals. Consequently, we must assume the presence of other signals besides NAO in the indices, especially in the monthly and seasonal indices since they have lower  $S/N$  ratios than does the winter-annual one.

The study of the cross-spectral characteristics of the two time series involved, through the study of the cross-spectral amplitude and phase-spectrum, can reveal the ranges of frequency at which the most important coherent simultaneous out-of-phase relationships take place. Based on this analysis, a convenient filter can be applied (in some cases) to remove these frequency ranges from the normalized pressure series prior to obtaining the NAO indices, thereby improving the significance of the indices as an indicator of the NAO. The filtering, ideally, should remove all signals at both stations that do not vary coherently in out-of-phase, but retain all simultaneous coherent out-of-phase variations; this eventually increases the  $S/N$ . Not only an increase in the  $S/N$  ratio is desirable, but also that the filtered series retains as much as possible of the variance of the original series. Thus, a compromise should be sought between the desired increase in the  $S/N$  ratio and variance retained. In all the cases, we have applied finite impulse response (FIR) digital filters based on the Kaiser window, with different orders depending on the series analysed. The choice of the order of a filter is a trade-off between the desired characteristic of the filter and the number of data we wish to lose. The Kaiser window is nearly optimum in the sense of having the greatest energy in the main lobe for a given peak side lobe level (Jackson, 1989). The filters constructed using this window are symmetric. A comprehensive review of these filters and their implementation can be found in King *et al.* (1989, chapter 2).

In the following sections, we analyse the cross-spectral characteristics of the three indices and propose several digital filters to improve the  $S/N$  ratio. Appendix A contains some brief notes on the cross-spectral analysis used in next sections.

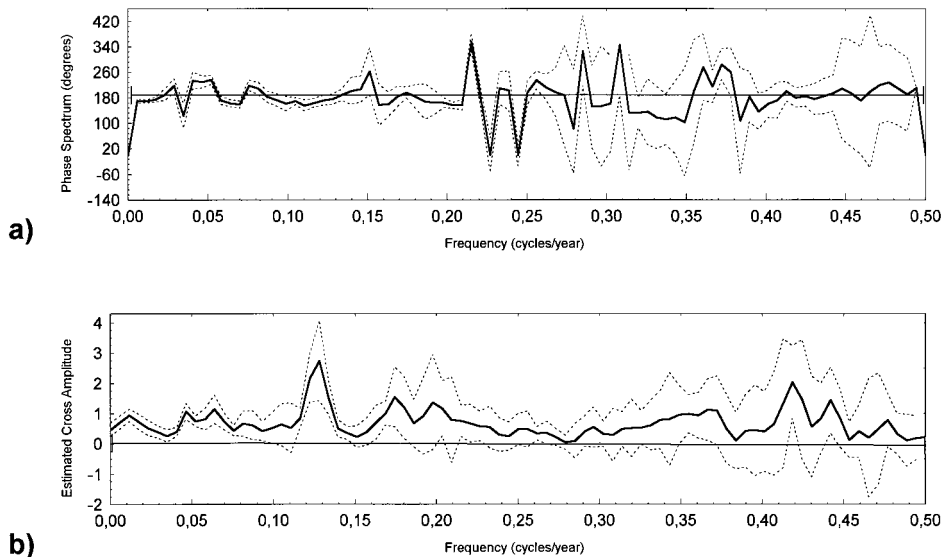


Figure 3. Estimated phase spectrum (a) and cross-amplitude (b), together with 90% confidence intervals calculating by jack-knifing, for the winter GI and IC indices. A Parzen window of width 7 has been used

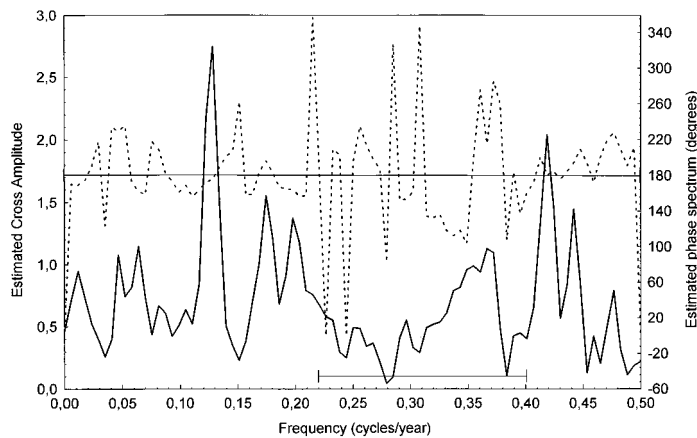


Figure 4. Estimated cross-amplitude and phase spectrum for the winter GI and IC indices. A substantial part of the coherent variations takes place in the range 0.1–0.2 cycles/years, with the major peak located around 0.12 cycles/year (8 years). Except for the range 0.22–0.40 cycles/year (highlighted with the segment) all the frequencies have associated, approximately, a 180° value in the phase spectrum

**3.3.1. Winter-annual index.** Figure 3 shows the cross-amplitude and phase spectrum for winter IC and GI normalized pressure data, together with 90% confidence intervals obtained by jack-knifing (Efron and Tibshirani, 1986, 1993). A Parzen window of width 7 (Percival and Walden, 1993) was used. Note the poor limits of both phase and cross-amplitude in the range 0.25–0.4 cycles/years and nearly 0.5 cycles/year, a consequence of the low cross-amplitudes. Figure 4 shows the cross-amplitude and phase spectrum in a single graph for the sake of comparison. Most important cross-amplitude peaks appear around 0.12 cycles/year (quasi-decadal mode); other major amplitudes are located around 0.42 and 0.17 cycles/year. Phase spectrum for all periods, except for the range 0.2–0.4 cycles/year, remain quite close to 180°, signifying that, for this range of periods, the variations in pressure at the northern and southern stations are approximately simultaneous and out-of-phase, and could be modelled using Equation (A3) (see Appendix A). Nevertheless, for the range 0.2–0.4 years, phase spectrum shows strong variations and a steep slope (indicative of some kind of lag–lead relationship between stations), which leads to the conclusion that, for this range of periods, the relationship between the northern and southern stations cannot be modelled using Equation (A3). Note the scarce power found at low frequencies.

The former analysis leads us to try several filters in order to improve the winter-annual NAO index in the sense of having a maximum  $S/N$  ratio but preserving as much as possible the out-of-phase coherent variance of the two stations. We filtered the series using, firstly, a band-pass filter for the band period 0.1–0.22 cycles/year and, secondly, using a cascade band-pass filter with band periods 0.1–0.22 and 0.4–0.5 cycles/year. We constructed both filters using a FIR Kaiser filters of order 7. The results are shown in Table IV. Although the  $S/N$  ratio was significantly improved with both filters, they retain only

Table IV. Correlation,  $S/N$  and variance (Var) of the NAO (GI–IC) and noise (GI+IC) indices calculated using the winter-annual anomalies pressure data of GI and IC after being passed through several filters

Filter (cycles/year)	Correlation	$S/N$	Var(GI–IC)	Var(GI+IC)
No filtering	–0.65	2.17	1.60	0.340
Band pass (0.10–0.22)	–0.78	2.90	0.19	0.023
Band pass (0.10–0.22) and (0.40–0.50)	–0.78	2.84	0.30	0.037
Stop-band (0.22–0.40)	–0.71	2.47	0.77	0.126

The stop-band over the 0.22–0.4 cycles/year band provides the best compromise between the increase in  $S/N$  and the retained variance after the filtering.

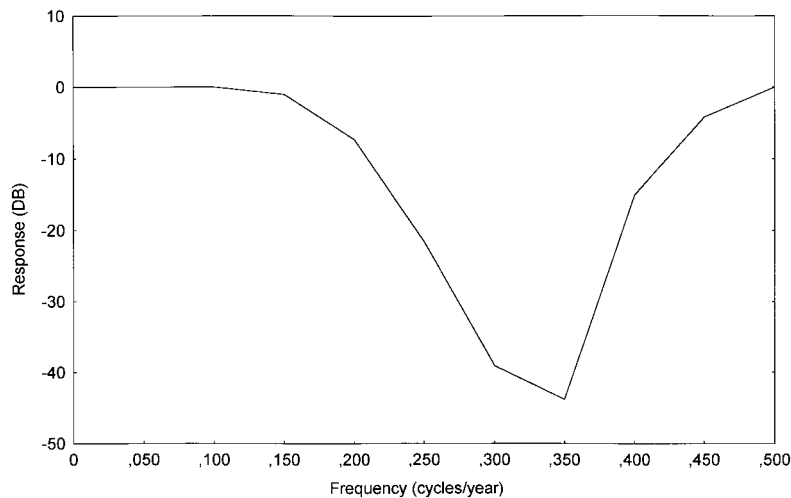


Figure 5. Response function  $[20 \log(|G(f)|^2)]$ ,  $G(f)$  being the gain of the filter] of the stop-band (0.22–0.4) cycles/year filter applied to the winter GI and IC indices

12.5% and 20%, respectively, of the original variance; a result that seems too severe. Since most of the incoherent out-of-phase signals occur in the range 0.22–0.40 cycles/year, we have applied a stop-band filter that removes the signals in this range. The improvement in the  $S/N$  ratio is also notable but the filter now retains 50% of the original variance. Figure 5 shows the response of the filter and Table V shows the weights of this filter. Finally, we selected this filter and applied it to the pressure anomaly series. Using these new anomalies with the band 0.22–0.40 cycles/year removed, we obtained a new NAO winter-annual index, which we will call hereafter filtered winter-annual index. The index constructed using the raw pressure anomalies (not filtered) will be called hereafter raw winter-annual index.

Figure 6 shows the raw and filtered NAO winter-annual index. Also, the noise (GI + IC) index is shown for both the raw and filtered pressure data. The same scale has been used for all the plots; a comparison of figures clearly shows the improvement in the  $S/N$  ratio. Figure 7 shows the raw and the filtered NAO index. In almost all cases, the filtered index shows the same NAO phase as the raw index, with the values being close to each other. Only in a few cases does the sign of the filtered and unfiltered series not agree, but in these cases both indices have values very close to zero. Also remarkable is the agreement in the extreme index values, indicating that most of these extreme values result from coherent and out-of-phase variations (i.e. the NAO signal).

The filtering process appears to reduce the variance of the white noise term in Equation (A4), reducing, therefore, the swamping effect of the random variations. This makes relationship (A3) more plausible for our data. Note that the filtered NAO index, retaining almost all the physically meaningful information contained in the pressure data, has an improved  $S/N$  ratio in comparison with the NAO raw index and, therefore, better represents the state of the NAO.

**3.3.2. Seasonal index.** The seasonal series at AZ shows a statistically significant autocorrelation pattern. An ARIMA(4, 0, 0) filter was applied to it and the residual time series was used to study the cross-spectral characteristics. Figure 8 shows the cross-amplitude and phase spectrum, together with the 90% confidence

Table V. Weights of the filter used in the winter-annual index

	Weight number							
	0	$\pm 1$	$\pm 2$	$\pm 3$	$\pm 4$	$\pm 5$	$\pm 6$	$\pm 7$
Weight	0.62000	0.13638	0.17147	-0.13268	0.00336	0.00550	0.00556	0.00119

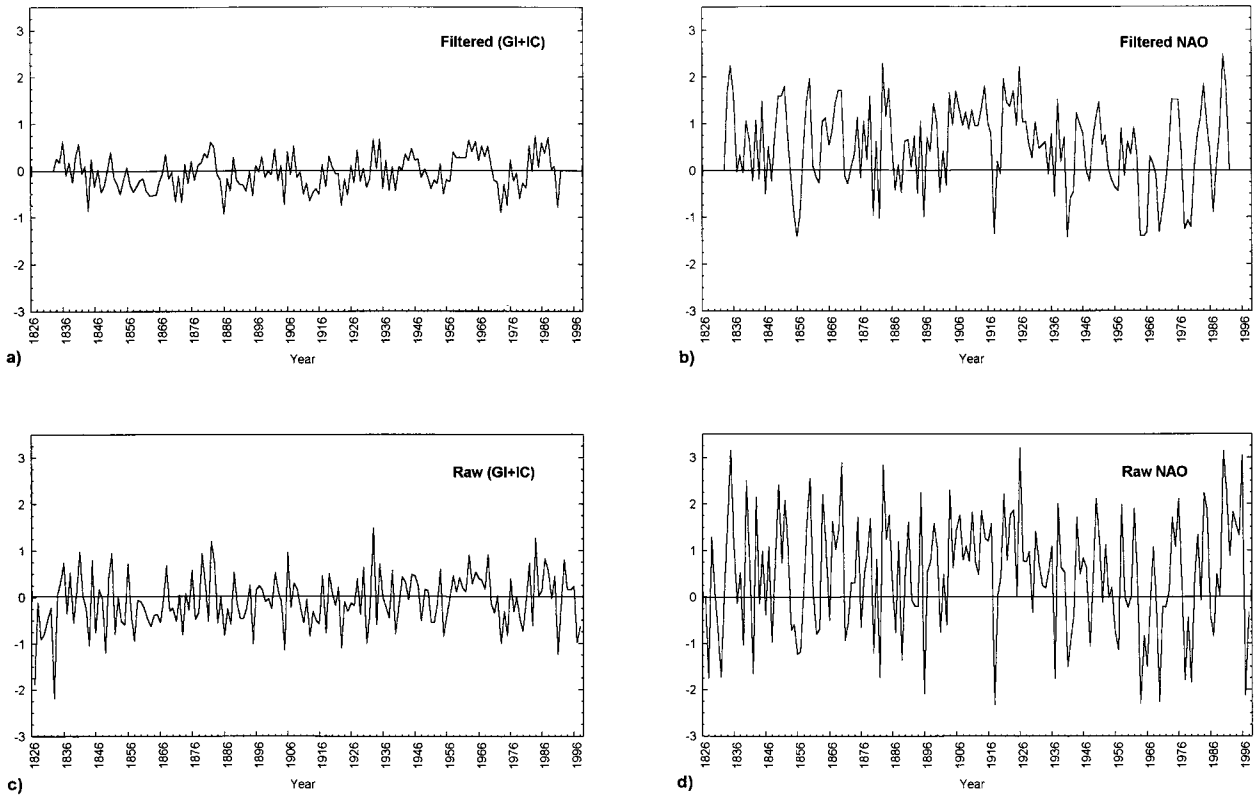


Figure 6. Plots of the NAO winter index (GI–IC) and noise (GI + IC) index using the filtered (a) and (b) and raw data (c) and (d). The improvement in the  $S/N$  ratio of the NAO index calculated using the filtered data in comparison with the index obtained using the raw data is easily seen

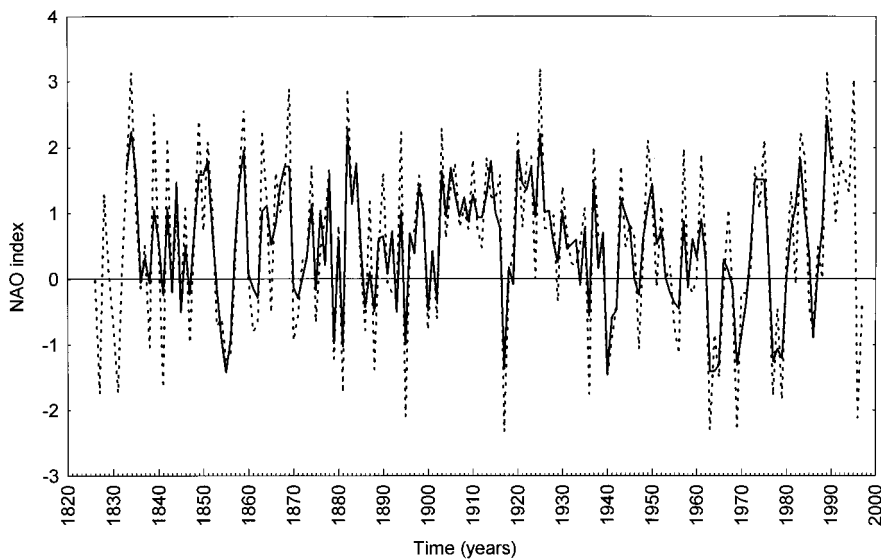


Figure 7. Raw winter-annual index (dashed line) and the filtered index obtained by removing the 0.22–0.40 cycles/year band (solid line). Note that in almost all the cases the filtered index shows the same NAO phase as the raw one

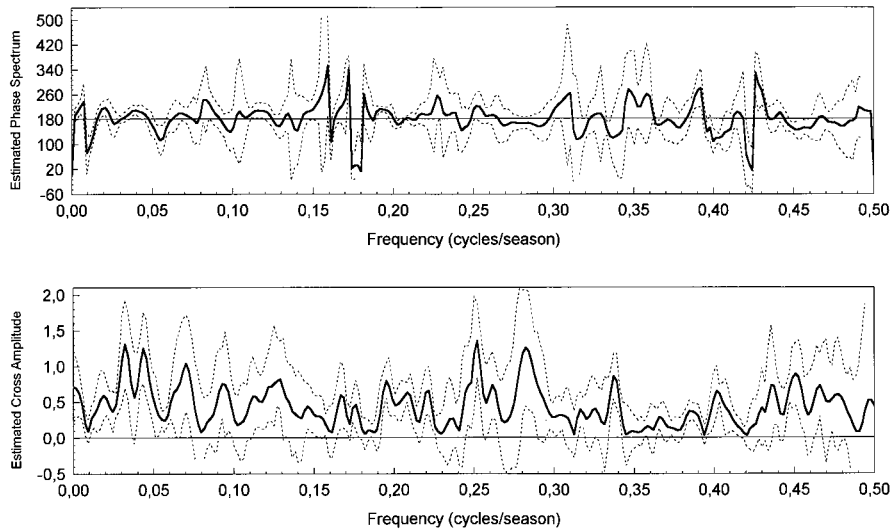


Figure 8. Estimated cross-amplitude and phase spectrum, along with 90% confidence intervals calculated by jack-knifing, for the seasonal AZ and IC indices. A Parzen window of width 11 has been used

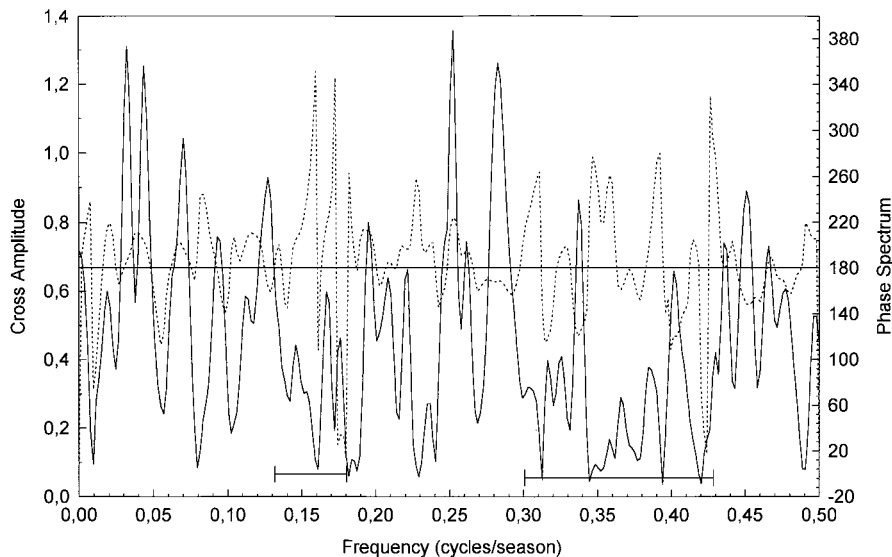


Figure 9. Estimated cross-amplitude and phase spectrum for the seasonal AZ and IC indices. Some characteristics are shared with the results of the winter analysis. Important coherent variations are located around 0.25 cycles/season (1 year) and 0.45 cycles/season (6 months) with an associated phase spectrum of  $180^\circ$ . Ranges of frequencies 0.13–0.18 and 0.30–0.43 (highlighted with the segments) are removed from the data prior to calculating the NAO seasonal index

interval obtained by jack-knifing, for the seasonal IC series and the residual time series of the AZ seasonal index. A Parzen window of width 11 was applied. Figure 9 shows both the cross-amplitude and the phase spectrum. The cross-spectrum in the seasonal case shows some different characteristics in comparison with those of the winter index, but the main features are shared. For instance, major peaks of coherent signals, with associated phase spectrum  $180^\circ$ , are found around frequency 0.03 cycles/season (8 years) and around 0.12 cycles/season (quasi-biennial), as in the case of winter; although now their importance is lessened. The lack of power in the range 0.22–0.40 cycles/year and their associated non-out-of-phase phase spectrum found in the winter case is not as pronounced in this case, as can be seen in Figure 9 (range

0.05–0.1 cycles/season). An additional feature of the seasonal case, which is not resolved in the winter-annual case, are strong coherent variations that occur in the range 0.2–0.3 cycles/season (i.e. quasi-annual) and around 0.45 cycles/season (roughly half a year). As a general characteristic, except for the ranges of frequencies (0.13–0.18) cycles/season (corresponding to 1.5–2 years) and (0.3–0.43) cycles/season (0.6–0.8 years), the phase spectrum seems to have a quite stable 180° value, and thus, Equation (A3) is valid.

We applied different filters, some of which are summarized in Table VI; all were constructed using Kaiser filters of order 12. The first filter was a band-pass on the frequencies 0–0.3 cycles/season; this filter did not improve the  $S/N$  ratio because in the range of frequencies 0.45–0.5 cycles/season there are significant coherent out-of-phase signals. We also applied two stop-band filters, the first in the range of frequencies 0.13–0.18 cycles/season; the second is a cascade type in the range of frequencies 0.13–0.18 and 0.30–0.43 cycles/season. As shown by the results in Table VI, this latter provides the best results, retaining around 58% of the original variance and significantly improving the  $S/N$  ratio. Finally, we chose this last filter and applied it to the seasonal anomalies pressure series in order to obtain a new NAO seasonal index, which we will call the seasonal filtered NAO index. As in the case of winter-annual index and for almost all the cases, the phase of the NAO is not changed when using the filtered data to construct the index. Furthermore, high values remain unchanged when using the filtered series, showing that these extreme values of the oscillation result from coherent out-of-phase variations.

**3.3.3. Monthly index.** As in the seasonal case, the AZ monthly series shows a significant autocorrelation pattern; thus an ARIMA(1, 0, 0) model was applied and the residual time series were used for the

Table VI. As in Table IV but for the seasonal AZ and IC anomalies

Filter (cycles/season)	Correlation	$S/N$	Var(AZ–IC)	Var(AZ+IC)
No filtering	–0.48	1.69	1.19	0.42
Band pass (0–0.30)	–0.47	1.68	0.74	0.26
Stop-band (0.13–0.18)	–0.49	1.72	0.89	0.30
Stop-band (0.13–0.18) and (0.30–0.43)	–0.55	1.86	0.69	0.20

The cascade stop-band on the frequency ranges 0.13–0.18 and 0.30–0.43 cycles/season provides the best results.

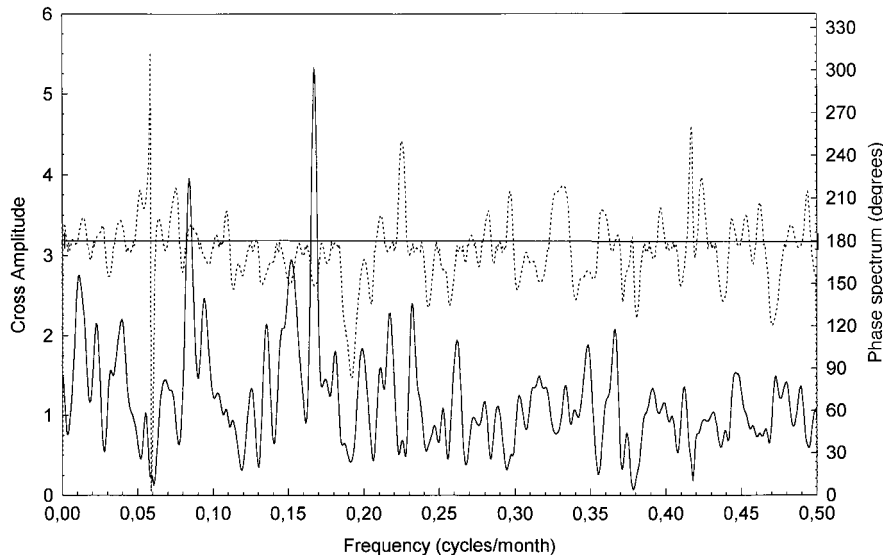


Figure 10. Estimated cross-amplitude and phase spectrum for the monthly AZ and IC indices. The most important peaks take place around 0.16 and 0.08 cycles/month (that correspond approximately to 6 months and 1 year quasi-periodicities). Frequencies greater than 0.18 cycles/month are removed from the monthly data prior to calculating the monthly NAO index

cross-spectral analysis. Figure 10 shows the cross-amplitude and the phase spectrum for the monthly IC series and AZ residual series, using a Parzen window of width 21. Confidence intervals obtained by jack-knifing (not shown) were wider for the range of high frequencies (higher than 0.2 cycles/month) due to the weak cross-amplitude in this range. Some characteristics common to those of the winter and seasonal cases were found. For instance, the most energetic cross-amplitude peaks appear at around 0.166 (6 months), 0.084 (1 year), 0.04 (quasi-biennial) and 0.011 cycles/month (7.5 years), although the power associated with these peaks appears to be weaker than in the winter and seasonal analyses. For all the frequencies in the range 0–0.18 cycles/month (except some spurious cases found at around 0.05 cycles/month due to the scarce power), relationship (A3) can be assumed to be valid.

Table VII shows the results of applying different band-pass filters to the monthly AZ and IC normalized pressure data, using Kaiser filters of order 20. Given the strong coherent out-of-phase variations that occur at around 0.166 cycles/month, the application of a band-pass filter that removes this signal results in a loss in the  $S/N$  ratio. The cross-amplitude associated with frequencies greater than 0.2 cycles/month are weak; the removal of this range slightly improves the  $S/N$  ratio. This analysis leads us finally to choose a band-pass 0–0.18 cycles/month filter, which removes all periods shorter than 6 months. This filter retains around 40% of the original variance and results in a  $S/N$  ratio of 1.81.

#### 4. SUMMARY AND CONCLUSIONS

Normalized pressure data from IC and GI (extending back to 1825) and AZ and LI (extending back to 1865) have been analysed in order to study the feasibility of using proxy indices to monitor the NAO at different time intervals (winter-annual, seasonal and monthly basis). Results shows that, if a monthly or seasonal index is required AZ must be selected as the southern station. The strongest correlation corresponds to the winter season using GI as the southern station, and thus, for the winter season, GI represents the southern part of the NAO dipole better than do AZ or LI. An analysis of the temporal stability of the correlation between stations reflects stability except for correlation between AZ and IC in summer; this correlation shows a trend toward lower values (less negative correlation) from 1920 onwards. The comparison of the proxy indices with the PC series of the NAO index defined by Barnston and Livezey (1987) globally confirms these findings. Furthermore, the best correlation between the ‘real’ NAO and the proxy indices is found during winter, followed by autumn and spring.

Cross-spectral analysis of winter-annual pressure data of the southern and northern stations shows that the most pronounced coherent out-of-phase variations between the two stations occur in periods of 2.5 years, 5–6 years and 8 years. The cross-spectral analysis of the seasonal and monthly series overall confirms these features found for the winter-annual case and shows some additional ones, such as the strong coherent variations at periods of around 6 months and 1 year. The use of two different and almost independent pressure datasets provide more confidence in the results. Additionally, the winter-annual data presents a considerable lack of power in the range 3–4 years, and the range 2.5–4.5 years does not correspond to a constant  $180^\circ$  value in the phase spectrum. Several studies have analysed the spectral characteristics of the NAO index. Rogers (1984) analysed the Fourier spectrum of the NAO winter index from 1900 to 1983, using pressure data from Iceland and The Azores islands, and found peaks at periods

Table VII. As in Table IV but for the monthly AZ and IC anomalies

Filter (cycles/month) (all band pass)	Correlation	$S/N$	Var(AZ–IC)	Var(AZ+IC)
No filtering	–0.49	1.68	3.16	1.16
(0–0.1800)	–0.53	1.81	1.24	0.38
(0–0.0840)	–0.47	1.67	0.56	0.20
(0.006–0.1800)	–0.53	1.79	1.17	0.36

Removing the range of frequencies greater than 0.18 cycles/month leads to a substantial gain in the  $S/N$  ratio.

of 5, 7 and 20 years. Hurrell and van Loon (1997), analysing the winter NAO index constructed using pressure data from LI and Stykkisholmur from 1865 to 1995, found significant variance at biennial periods and in the range 6–10 years, but a deficit of power in the 3–5-year range, in close agreement with our results. In a recent study, Appenzeller *et al.* (1998) using wavelet transform to analyse a proxy NAO annual index of 350 years, found highly non-stationary behaviour in the NAO index, the maximum power being concentrated in periods of less than 15 years.

Results from cross-spectral analysis must be treated with caution when analysing, as in our case, short and noisy time series (Yiou *et al.* 1996; Wunsch, 1999). Nevertheless, the use of the pre-whitening procedure, as in our case, provides certain confidence in the results.

Based on the cross-spectral analysis, the pressure data was filtered prior to constructing the NAO indices in order to improve the  $S/N$  ratio. In the case of seasonal index, the  $S/N$  ratio using filtered data is 1.9 (1.69 using unfiltered data), retaining 58% of the original variance. For the case of the monthly index, the filtered data lead to an  $S/N$  ratio of 1.8 (1.68 using unfiltered data), retaining 40% of the original variance. Finally, for the winter index, the  $S/N$  is 2.47 (2.16 using unfiltered data), retaining 50% of the original variance. The comparison of the filtered and unfiltered indices reveals certain features. For the three indices, especially in the winter-annual index, the new index based on the filtered data has the same NAO phase as the original one for almost all the cases. Furthermore, when an extreme value of the oscillation is present in the unfiltered NAO index, in almost all the cases, this extreme value is also present when using the filtered series to construct the NAO index. These two facts indicate that even the use of the data without filtering leads to an NAO index that contains appreciable physical information. In particular, extreme events of the oscillations seem to be associated with coherent and out-of-phase variations between the pressure at the northern and the southern centre of the NAO dipole. The filtering procedure removes part of the data at the beginning and end of the series (depending on the order of the filter), and, therefore, the use of the filtering in an operational sense is limited. Nevertheless, filtered indices could be useful for a more reliable value of the NAO.

#### ACKNOWLEDGEMENTS

The Spanish CICYT, Project CLI98-0930-CO2-01, financed this work. The authors would like to thank Dr Phil Jones (Climatic Research Unit, University of East Anglia, UK) for providing the pressure data from Gibraltar, Iceland and The Azores and for the helpful comments made during David Pozo's stay at the Climatic Research Unit. Thanks also to Dr James Hurrell (National Center for Atmospheric Research, Boulder, CO, USA) for providing the pressure data from Lisbon. NAO index based on gridded SLP data were obtained from the National Center for Environmental Prediction (NCEP). The authors also want to thank Professor J.M. Angulo (Statistics Department of the University of Granada) very much for valuable discussions concerning the statistical procedures used in this work. Thanks also to the reviewers for their very valuable comments on the paper.

#### APPENDIX A

##### A.1. ARIMA models

This section provides a brief review on ARIMA models, including definition and modelling guidelines and comments on the software routines used. Statistical software package S-plus (StatSci, 1995) has been used. A comprehensive review can be found in Hipel and McLeod (1994) and Brockwell and Davis (1996).

A stochastic process  $\{X_t\}$ , with mean zero, has an ARIMA( $p, 0, q$ ) stationary (known as ARMA ( $p, q$ )) representation when it can be expressed in the form

$$X_t - \phi_1 X_{t-1} - \phi_2 X_{t-2} - \cdots - \phi_p X_{t-p} = a_t - \theta_1 a_{t-1} - \theta_2 a_{t-2} - \cdots - \theta_q a_{t-q} \quad (\text{A1})$$

where  $\{a_t\}$  is a white noise Gaussian process (normality is not generally necessary) with variance  $\sigma_a^2$  and zero mean;  $p$  and  $q$  are non-negative integers,  $\{\phi_1, \dots, \phi_p\}$  are the autoregressive (AR) coefficients and  $\{\theta_1, \dots, \theta_q\}$  are the moving average (MA) coefficients.

The model is selected, studying the autocorrelation function (ACF) and the partial autocorrelation function (PACF). To ensure a physically meaningful model for our time series, some constraints (concerning the stationarity and invertibility) must be imposed on the parameters of the model, and some consideration concerning the parsimony must be taken into account. Besides this, a candidate model must have a white noise process as a residual time series. In our analysis, we have used a Pormanteau test developed by Ljung and Box (1978). We have used the Akaike Information Criterion (AIC) (Akaike, 1974) to select the final model from the models available. The AIC is based on information theory and represents a compromise between the goodness of the fit and the number of parameters of the model. The model with minimum AIC value should be selected.

#### A.2. Study of the inter-dependence between time series: pre-whitening and cross-spectral analysis

Given two stationary stochastic processes  $\{X_t\}$  and  $\{Y_t\}$ , their inter-dependence can be studied through the cross-correlation function (CCF) (Pierce and Haugh, 1977), defined as

$$\rho_{xy}(k) = \gamma_{xy}(k) / \{\gamma_{xx}(0)\gamma_{yy}(0)\}^{1/2}, \quad k = -j, -j+1, \dots, j, \quad (\text{A2})$$

where  $\gamma_{xy}(k) = \text{Cov}\{X_t, Y_{t-k}\}$  is the CCF.

Given two real time series  $\{x_t: t = 1, 2, \dots, n\}$  and  $\{y_t: t = 1, 2, \dots, n\}$ , a sample estimator of the CCF from the data can be used. However, if the two series are themselves auto-correlated, the study of their relationship by means of the estimated CCF can lead to misleading conclusions (Hipel and McLeod, 1994, chapter 16); sampling variability can lead to large sample cross-correlation values at some lag, which standard tests incorrectly identify as being significantly different from zero. To alleviate this problem, the series could be transformed prior to the correlation analysis. Such a transformation must remove the autocorrelation of the time series, but should allow the transformed series to maintain the same relationship as that of the original series. ARIMA transformations belong to this kind of transformation. ARIMA filters can be used to remove the autocorrelation, transforming the series so that it resembles a white noise process. Because of the linear nature of ARIMA models, the residuals of the transformed series and the original series are related in the same way. Transformation of observed series to resemble white noise prior to evaluation of their inter-dependence is called pre-whitening. A reliable significance estimation of the CCF can be assessed if the pre-whitened series are used (Haugh, 1976). Katz (1988) shows an analysis of the advantages of using the pre-whitening procedure in climatic time series.

Although the time and frequency domain representations of time series are formally equivalent, the frequency domain can provide more insight in certain situations than can the time domain and vice versa. Particularly, cross-spectrum analysis can be used as a complement to cross-correlation analysis in the time domain in order to study the relationship between time series.

Using cross-spectral analysis, it is possible to determine for which frequency ranges the pressure at the northern and southern stations undergoes approximately simultaneous coherent out-of-phase variations. Given the pressure data at the northern  $\{n_t: t = 1, \dots, n\}$  and southern  $\{s_t: t = 1, \dots, n\}$  station, it is possible to ascertain for which range of frequencies the following approximate formula can be assumed:

$$n_t \approx -s_t. \quad (\text{A3})$$

Let us assume that  $\{S_t\}$  is a stationary process with auto-covariance function  $\gamma_{xx}(k)$  and spectrum

$$f_{xx}(w) = \sum_{k=-\infty}^{k=+\infty} \gamma_{xx}(k) e^{-ikw}.$$

Let  $\{N_t\}$  be defined by

$$N_t = -S_t + a_t, \quad (\text{A4})$$

where  $\{a_t\}$  is a white noise process with variance  $\sigma_a^2$ . Note that  $\{N_t\}$  and  $\{S_t\}$  could represent the pressure at two localized stations (the northern and southern centre of the NAO dipole).

It can be shown (Diggle, 1990, p. 213) that, for this bivariate process, coherency is given by

$$b_{xy}(w) = \{1 + \sigma_a^2/f_{xx}(w)\}^{-1/2}$$

and the phase spectrum is

$$\Phi_{xy} = \pi.$$

Here, the form of the phase spectrum makes intuitive sense, since the constant value  $\pi$  radians corresponds to the simple change of sign in Equation (A3). The coherency is small if  $\sigma_a^2$  is large and vice versa, depending on whether the relationship between the series is or is not overwhelmed by the random variations in the white noise sequence. Thus, the range of frequencies for which relationship (A3) can approximately be assumed may be determined by studying the phase spectrum of the data.

Note that the cross-spectrum is obtained as the discrete Fourier transform of the CCF and thus any problem that concerns the estimates of the cross-covariance also affects the cross-spectrum estimates. A pre-whitening procedure is also necessary prior to obtaining the cross-spectrum when autocorrelation is evident in the data.

#### REFERENCES

- Akaike H. 1974. A new look at the statistical model identification. *IEEE Transactions on Automated Control* **19**: 716–723.
- Appenzeller C, Stocker TF, Anklin M. 1998. North Atlantic Oscillation dynamics recorded in Greenland ice cores. *Science* **282**: 446–450.
- Barnston AG, Livezey RE. 1987. Classification, seasonality and persistence of low-frequency atmospheric circulation patterns. *Monthly Weather Review* **115**: 1083–1126.
- Brockwell PJ, Davis RA. 1996. *Introduction to Time Series and Forecasting*. Springer: Berlin; 420.
- Davis RE, Hayden B, Gay D, Phillips W, Jones G. 1997. The North Atlantic subtropical anticyclone. *Journal of Climate* **10**: 728–744.
- Diggle PJ. 1990. *Time Series. A Biostatistical Introduction*. Oxford University Press: Oxford; 257.
- Efron B, Tibshirani RJ. 1986. The bootstrap method for standard errors, confidence intervals, and other measures of statistical accuracy. *Statistical Science* **1**: 1–35.
- Efron B, Tibshirani RJ. 1993. *An Introduction to the Bootstrap*. Chapman & Hall: London; 435.
- Haugh LD. 1976. Checking the independence of two covariance-stationary time series: a univariate residual cross-correlation approach. *Journal of the American Statistical Association* **71**: 378–385.
- Hipel KW, Mcleod AI. 1994. *Time Series Modelling of Water Resources and Environmental Systems*. Elsevier: Amsterdam; 1013.
- Hurrell JM. 1995. Decadal trends in North Atlantic Oscillation and relationship to regional temperature precipitation. *Science* **269**: 676–679.
- Hurrell JM. 1996. Influence of variations in extratropical wintertime teleconnections on Northern Hemisphere temperatures. *Geophysical Research Letters* **23**: 665–668.
- Hurrell JM, van Loon H. 1997. Decadal variations in climate associated with the North Atlantic Oscillation. *Climatic Change* **36**: 301–326.
- Jackson LB. 1989. *Digital Filters and Signal Processing*. Kluwer Academic: Dordrecht; 410.
- Jones PD, Jonsson T, Wheeler D. 1997. Extension to the north Atlantic Oscillation index using early instrumental pressure observations from Gibraltar and southwest Iceland. *International Journal of Climatology* **17**: 1–18.
- Jones PD, Wigley TML, Briffa KR. 1987. Monthly mean pressure reconstruction for Europe (back to 1780) and North America (to 1858). US Department of Energy, Carbon Dioxide Research Division Technical Report TR038.
- Kapala A, Mächel H, Flohn G. 1998. Behaviour of the centres of action above the Atlantic since 1881. Part II: associations with regional climate anomalies. *International Journal of Climatology* **18**: 23–36.
- Katz RW. 1988. Use of cross correlation in the search for teleconnections. *Journal of Climatology* **8**: 241–253.
- King R, Ahmadi M, Gorgui-Naguib R, Kwabwe A, Azimi-Sadjadi M. 1989. *Digital Filtering in One and Two Dimensions. Design and Applications*. Plenum Press: New York; 466.
- Ljung GM, Box GE. 1978. On a measure of lack of fit in time series models. *Biometrika* **65**: 297–303.
- Mächel H, Kapala A, Flohn G. 1998. Behaviour of the centres of action above the Atlantic since 1881. Part I: characteristic of seasonal and interannual variability. *International Journal of Climatology* **18**: 1–22.
- Moses T, Keladis G, Diaz HF, Barry R. 1987. Characteristic and frequency of reversal in mean sea level pressure in the North Atlantic sector and their relationship to long-term temperature trends. *International Journal of Climatology* **7**: 13–30.
- Osborn TJ, Briffa K, Tett SFB, Jones PD, Trigo RM. 1999. Evaluation of the North Atlantic Oscillation as simulated by a climate model. *Climate Dynamics* **15**: 685–702.
- Percival BP, Walden AT. 1993. *Spectral Analysis for Physical Applications, Multitaper and Conventional Univariate Techniques*. Cambridge University Press: Cambridge; 583.
- Pierce DA, Haugh LD. 1977. Causality in temporal systems. *Journal of Econometrics* **5**: 265–293.

- Rogers JC. 1984. The association between the North Atlantic Oscillation and the Southern Oscillation in the Northern Hemisphere. *Monthly Weather Review* **112**: 1999–2015.
- Rogers JC, van Loon H. 1979. The seesaw in winter temperatures between Greenland and Northern Europe. Part II: some oceanic and atmospheric effects in middle and high latitudes. *Monthly Weather Review* **107**: 509–519.
- Ropelewski CF, Jones PD. 1987. An extension of the Tahiti–Darwin Southern Oscillation Index. *Monthly Weather Review* **115**: 2161–2165.
- Shasmanoglou HS. 1990. A contribution to the study of the action centres in the North Atlantic. *International Journal of Climatology* **10**: 247–261.
- StatSci. 1995. *S-Plus Guide to Statistical and Mathematical Analysis. Version 3.3*.
- Trenberth KE. 1984. Signal versus noise in the Southern Oscillation. *Monthly Weather Review* **112**: 327–333.
- Trenberth KE. 1995. Atmospheric circulation climate changes. *Climatic Change* **31**: 427–453.
- Wallace JM, Gutzler DS. 1981. Teleconnections in the geopotential height field during the Northern Hemisphere winter. *Monthly Weather Review* **109**: 784–812.
- Wunsch C. 1999. The interpretation of short climate records, with comments on the North Atlantic and Southern Oscillations. *Bulletin of the American Meteorological Society* **80**: 245–255.
- Yiou P, Baert E, Loutre MF. 1996. Spectral analysis of climate data. *Surveys in Geophysics* **17**: 619–663.